

Incorporating Uncertainty in Learning to Defer Algorithms for Safe Computer-Aided Diagnosis

Jessie Liu^{1*}, Blanca Gallego¹, Sebastiano Barbieri¹

¹Centre for Big Data Research in Health, University of New South Wales

Introduction

Neural networks with multiple hidden layers (deep learning algorithms) are increasingly being applied to electronic medical records, clinical notes, and medical images for diagnostic purposes. Computer-aided diagnosis has the potential to reduce erroneous decisions and the resource burden imposed on clinical staff. Nevertheless, the use of deep learning for automation in healthcare remains troublesome [1], because of the limited interpretability of these methods and because erroneous diagnoses or predictions can be extremely costly for patients [2].

A simple approach to limit the number of erroneous computer-aided diagnoses consists in trusting the model's predictions only if the associated output probabilities are above a specified threshold, but this is problematic due to the poor calibration of deep neural networks [3]. An alternative approach consists of automating the diagnosis of a patient only if the expected model error is lower than the expected human error [2]. The expected model error can be determined by calibrating the output probabilities, or by training an auxiliary neural network to predict the probability of a wrong diagnosis based on the patient's input data. The human error can be estimated by assessing the clinician's accuracy on similar, previously seen, patients, or by building another neural network which predicts the probability of experts' disagreement regarding a patient's diagnosis [4].

Another recent stream of research, including learning with rejection [5] and learning to defer methods [6][7], proposes to build neural networks which identify groups of patients whose diagnosis can be automated with high accuracy. Learning with rejection [5] simultaneously learns a classifier for the diagnostic task at hand and a rejection function. Such an approach is effective when the optimal rejection region cannot be defined as a simple function of the predicted diagnoses. Learning to defer [6][7] considers the model and human decision makers together to optimize the system's overall accuracy. It does this by automatically diagnosing groups of patients for whom the model is highly accurate and, at the same time, deferring the remaining patients for evaluation by a human expert. Two different approaches have been suggested to combine computer-aided and human diagnoses: one approach starts by training a neural network to predict either the diagnostic class or a binary defer indicator; deferred patients are then passed to human decision makers who might have access to additional patient information or domain expertise [6]. Another approach also trains a neural network to either diagnose or defer, but includes the cost of deferring decisions to human experts within the network's loss function. Specifically, the loss function is the sum of two terms: a classification loss term and a defer loss term [7]. When diagnoses by human experts on the training data are not available, the cost of deferring to experts can be assumed to be constant [7], and the problem becomes to learn a classifier and a defer indicator in one training process.

In this study we propose the Learning to Defer with Uncertainty (LDU) algorithm which considers the diagnostic network's predictive uncertainty when learning which patients to diagnose automatically and which patients to defer to human experts. Our aim is to minimize patients' risk when machine learning

* Correspondence to jessie.liu1@unsw.edu.au

(ML) models are deployed in healthcare settings, by preventing the application of computer-aided diagnoses in groups of patients for whom the expected diagnostic error is large. We demonstrate that in situations where prior estimates of human error or human cost are not available, the LDU algorithm reduces the proportion of patients deferred for human evaluation, while achieving the same performance as previously proposed ‘learning to defer’ methods.

Method

The LDU algorithm consists of two stages (illustrated in Figure 1): in stage one an ensemble of neural networks is trained for the diagnostic task at hand, and diagnoses are determined for every patient with associated uncertainty measures; in stage two a ‘learning to defer’ neural network takes as input the predicted diagnoses and uncertainty measures from stage one and outputs either the patient’s diagnosis or the decision to defer to a human expert.

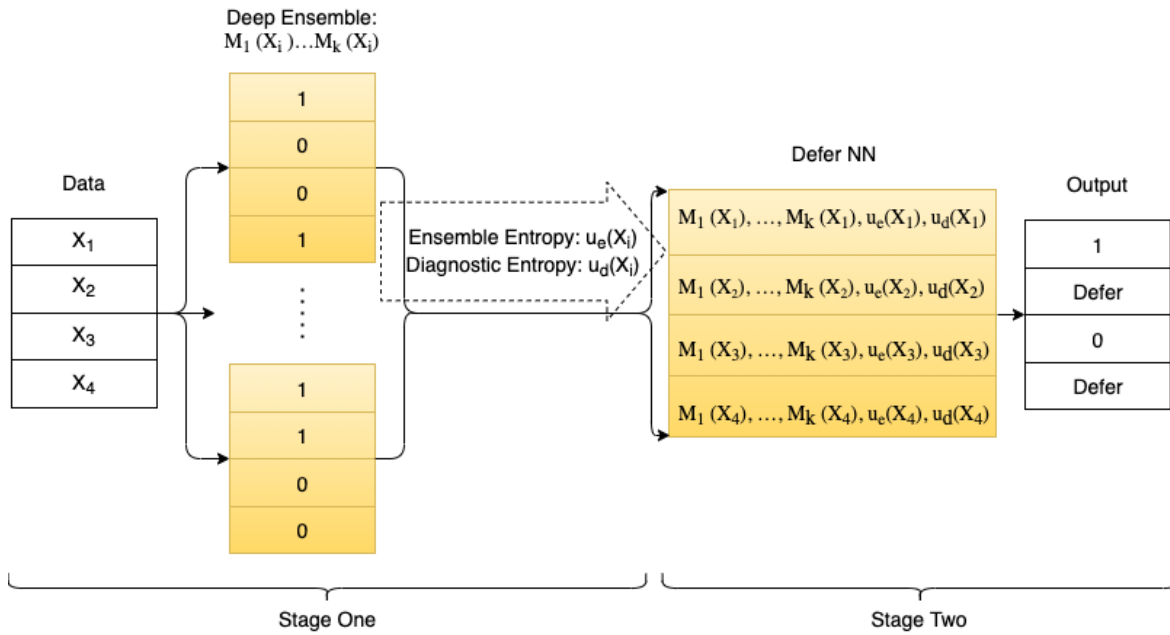


Figure 1. Learning to defer using ensemble predictions and their entropy.

There are two sources of uncertainty for a ML model: aleatoric uncertainty (caused by the inherent noise in the observed data) and epistemic uncertainty (associated with the distribution of the model’s parameter values). Both sources of uncertainty impact the probability distribution of predicted diagnoses; however, aleatoric uncertainty is generally more difficult to quantify because of the lack of multiple measurements of the same variable. Deep ensembles, i.e. ensembles of deep neural networks trained with different random initializations [9], have been found sufficient for capturing epistemic uncertainty, without the need for additional bootstrapping of the training data. In this study epistemic uncertainty is quantified by computing both the entropy of the continuous probabilities computed by a deep ensemble (denoted as ‘ensemble entropy’) and the entropy of the expected probabilities for each diagnosis (denoted as ‘diagnostic entropy’) [8]

More formally, the ensemble entropy is calculated as:

$$u_e(x_i) = - \sum_{k=1}^K P_k(x_i) \log P_k(x_i) \quad (I)$$

where K is the number of deep neural networks in the ensemble and $P_k(x_i)$ is the probability of a positive diagnosis computed by the k -th neural network based on patient data x_i .

Similarly, the diagnostic entropy is calculated as:

$$u_d(x_i) = -\sum_{c=1}^C P_c(x_i) \log P_c(x_i) \quad (\text{II})$$

where C is the number of classes ($C=2$ for binary classification) and $P_c(x_i)$ is the fraction of neural networks in the ensemble that predict that input x_i belongs to class c . The more evenly the deep ensemble predictions are distributed between positive and negative classes, the larger the diagnostic entropy will be, which represents higher uncertainty.

In stage two, a learning to defer neural network is built. The network takes as input the output probabilities of the deep ensemble ($M_1(x_i), M_2(x_i), \dots, M_k(x_i)$) and the associated ensemble entropy and diagnostic entropy, for a total of $K+2$ inputs. It outputs either the predicted diagnostic class or the defer class: $f(M_1(x_i), M_2(x_i), \dots, M_k(x_i), u_d(x_i), u_b(x_i)) = \text{class}_{c \in (1, \dots, C)} \text{ or defer}$

The learning to defer network was trained using a previously described loss function [7]. This loss function includes two terms: a cross-entropy loss with the *target* ($\text{class}_{c \in (1, \dots, C)}$), and a weighted cross-entropy loss with the *defer* class. With $j \in (\text{class}_1, \dots, \text{class}_C, \text{defer})$, the loss can be described as in Equation (III). The parameter α is used to adjust the weight of samples that the model decides to defer: by decreasing α , the network is encouraged to defer patients for human evaluation, and vice versa.

$$\text{loss}(x, \text{target}, \text{defer}) = -\log\left(\frac{\exp(x[\text{target}])}{\sum_j \exp(x[j])}\right) - \alpha \log\left(\frac{\exp(x[\text{defer}])}{\sum_j \exp(x[j])}\right) \quad (\text{III})$$

Our proposed LDU algorithm was tested on three diagnostic tasks¹ using different types of medical data: (1) diagnosis of myocardial infarction using free-text discharge summaries from the MIMIC-III database², (2) diagnosis of any comorbidities (positive Charlson Index) using structured hospital records from the Heritage Health dataset³ (this diagnostic task has been used previously to evaluate in learning to defer methods [6]), and (3) diagnosis of pleural effusion and diagnosis of pneumothorax using chest x-ray images from the MIMIC-CXR database⁴.

Data Sources and Processing

Diagnosis of myocardial infarction: Discharge summaries for ICU patients at Beth Israel Deaconess Medical Center in Boston, MA, USA, publicly available in the MIMIC-III² database [10], were used for the diagnosis of myocardial infarction (MI). Patients were assigned to the positive group if they had a discharge diagnosis of myocardial infarction (ICD codes starting with 410) at the end of a hospital stay. There were 6,183 discharge summaries for patients with MI and 51,093 discharge summaries for the negative group. To address the imbalance between patients with and without MI, the group of patients without MI was down sampled to 6,183. The free text data were pre-processed by removing de-identification expressions and format characters, and tokenized using the bio discharge summary BERT tokenizer [11]. Long discharge summary notes were split into sequences, with 512 token representations in each sequence.

¹ <https://github.com/liu-res/Learning-to-Defer-with-Uncertainty>

² <https://physionet.org/content/mimiciii/1.4/>

³ <https://www.kaggle.com/c/hhp>

⁴ <https://physionet.org/content/mimic-cxr/2.0.0/>

Diagnosis of any comorbidities: The Heritage Health dataset³, a structured dataset provided by the Heritage Provider Network (HPN) and containing data of members over a 48-month period, was used to predict the presence of any comorbidities (positive Charlson Index). Features extracted for 21361 members included demographic information (age and sex), claim information such as length of hospital stays, primary condition groups, procedure groups, and number of drug prescriptions and laboratory values and days since first services. Members with a positive Charlson Index for any claim were assigned to the group with comorbidities, all others were assigned to the negative group. The majority class was down sampled to have the same number of members within each class, this resulted in 14726 members in the dataset.

Diagnosis of pleural effusion and pneumothorax: Chest x-ray images from the MIMIC-CXR⁴ database were used for two diagnostic tasks: the diagnosis of pleural effusion and the diagnosis of pneumothorax. The dataset provides ground truth diagnoses for the two conditions and metadata including view positions [14]. Two datasets were derived for the two diagnostic tasks in the following manner: at first patients were divided into non-overlapping positive and negative groups depending on whether they had at least one positive chest x-ray. Then, anteroposterior (AP) view images were selected for every patient and the majority class was down sampled. The process resulted in 17,102 images for the pleural effusion dataset, and 15,838 images for the pneumothorax dataset.

For all diagnostic tasks, the data was split into training and testing datasets based on a 70-30 ratio.

Diagnostic Neural Networks

Three different types of neural networks were developed for each diagnostic task in this study (Appendix A). These diagnostic networks were used in the first stage of the proposed LDU algorithm (as deep ensembles), as well as to develop baseline algorithms for comparison with the LDU algorithm.

LDU Parameters

The deep ensembles for stage one of the LDU approach consisted of 50 randomly initialized diagnostic neural networks. The learning to defer neural network in stage two of the LDU approach was fully connected with two hidden layers (100 nodes each). For the myocardial infarction, pleural effusion and pneumothorax diagnostic tasks, the network was trained over 20 epochs using stochastic gradient descent with a learning rate of $5e-5$. For the comorbidity prediction task, the network was trained over 20 epochs using an ADAM optimizer with a learning rate of $9e-4$.

Baseline Algorithms

The proposed LDU algorithm was compared against two triage algorithms: learning to defer (without uncertainty information) and direct triage by uncertainty.

Learning to Defer (Without Uncertainty Information)

Previously proposed learning to defer algorithms do not consider uncertainty information [6][7]. For every task, learning to defer networks were developed by modifying the corresponding diagnostic neural networks: the output size of the network was increased by one, i.e. if the original binary classification outputs were 0 and 1, the modified outputs were 0, 1 and 2 (defer class). The loss function in Equation (III) was used for training. Adjusting α of the defer loss leads to different trade-offs between model performance and defer rates.

Direct triage by uncertainty

For each diagnostic task, deep ensembles [9] consisting of 50 randomly initialized diagnostic neural networks were trained. Predictive uncertainty was estimated by calculating the diagnostic entropy for every patient. Patients whose diagnostic entropy was above a specified threshold were deferred to human experts. Adjusting the probability threshold leads to different trade-offs between model performance and defer rates. Diagnostic entropy (entropy of the expected probabilities for each diagnosis) was used instead of ensemble entropy (entropy of the ensemble output probabilities), because of its superior performance (Appendix B).

Evaluation

We compare the performance between (1) the proposed LDU algorithm, (2) learning to defer without considering predictive uncertainty information [6][7], and (3) direct triage by uncertainty. Two types of F1 scores were computed for every model: an F1 score for patients who were not deferred to a human expert (denoted as “F1” for simplicity), and an overall F1 score for the entire patient group, by assuming that patients who are deferred to a human expert all receive the correct diagnosis (“F1 Overall”). The F1 score of the diagnostic neural network (without defer option) is reported as well (denoted as "Diagnostic Network F1"). We systematically varied the α (weight of defer loss) for methods (1) and (2) and the entropy threshold for method (3) in training, to achieve F1 scores for non-deferred patients above the diagnostic network F1 scores, and measured the corresponding defer rates. Furthermore, performance metrics including accuracy, sensitivity, specificity were compared between LDU and learning to defer without uncertainty for selected arbitrary F1 scores.

Results

Diagnosis of myocardial infarction

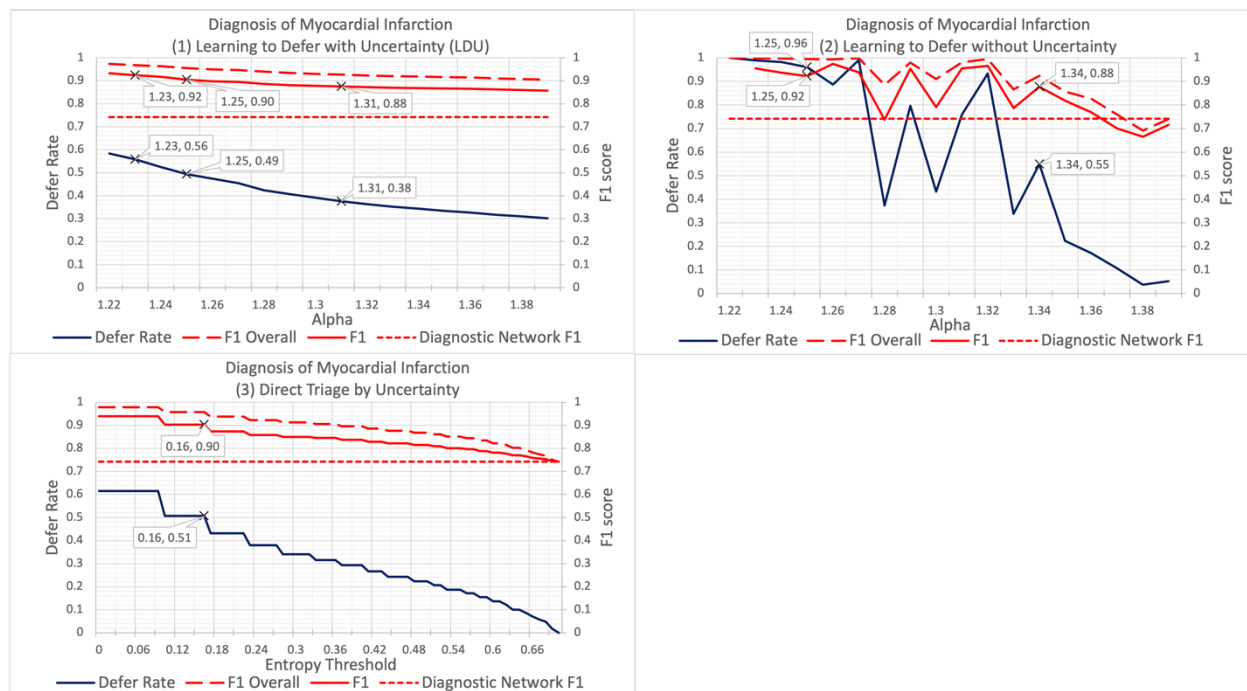


Figure 2. Performance comparison for the diagnosis of myocardial infarction using MIMIC-III discharge summaries and the following algorithms: (1) Learning to defer with uncertainty (LDU), (2) Learning to defer without uncertainty information, (3) Direct triage by uncertainty. Each panel shows the F1 scores (red line) for patients who are not deferred to human experts, ‘F1 Overall’ scores (red dashed line) and the corresponding defer rates (blue line) for different values of the weight of the defer loss α (methods (1) and (2)) or of the entropy threshold (method (3)). The diagnostic network F1 score (without the defer option) is 0.74 (red dotted line).

Figure 2 shows that to achieve an F1 score of 0.90 in the diagnosis of myocardial infarction, the LDU algorithm defers a slightly lower proportion of patients than the direct triage algorithm (49% vs 51%, respectively). However, the LDU algorithm may defer considerably less patients than learning to defer without uncertainty: e.g. to achieve an F1 score of 0.88 (an approximately 20% increase over the diagnostic network’s F1 score), the LDU algorithm defers only 38% of patients while learning to defer without uncertainty defers 55% of patients.

Importantly, the F1 scores and defer rates of the LDU and triage by uncertainty algorithms increase monotonically as the weight α of the defer loss or the entropy threshold are decreased. Specifically, as α is reduced from 1.31 to 1.23, LDU’s defer rate increases from 38% to 56%, and meanwhile the F1 score increases monotonically from 0.88 to 0.92. This is not the case for learning to defer without uncertainty: even though it is possible to achieve the same F1 score when α equals 1.25, the defer rate and F1 score fluctuate as α decreased. This indicates that higher F1 scores can be expected as more patients are deferred for the LDU and direct triage algorithms but not necessarily for learning to defer without uncertainty.

In summary, the LDU and direct triage algorithms performed similarly well on this diagnostic task, with results suggesting that the weight of the defer loss or the entropy threshold can be adjusted during training to achieve the desired trade-off between performance and defer ratio.

Diagnosis of any comorbidities

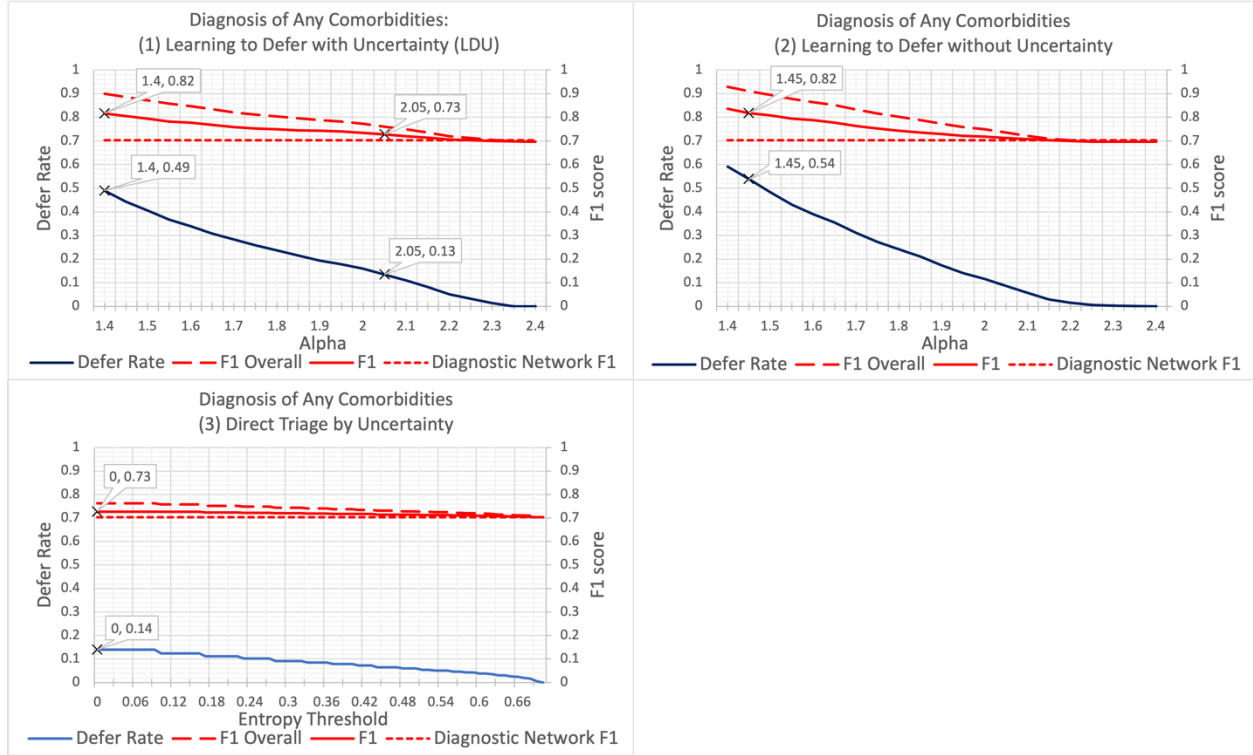


Figure 3. Performance comparison for the diagnosis of any comorbidities (identified by positive Charlson Index) using the Heritage Health dataset and the following algorithms: (1) Learning to defer with Uncertainty (LDU), (2) Learning to defer without uncertainty information, (3) Direct triage by uncertainty. Each panel shows the F1 scores (red line) for patients who are not deferred to human experts, ‘F1 Overall’ scores (red dashed line) and the corresponding defer rates (blue line) for different values of the weight of the defer loss α (method (1) and method (2)) or of the entropy threshold (method (3)). The diagnostic network F1 score (without the defer option) is 0.70 (red dotted line).

Figure 3 shows that to achieve an F1 score of 0.82 in the diagnosis of any comorbidities (an approximately 17% increase over the diagnostic network’s F1 score), learning to defer without uncertainty defers 54% of patients for human evaluation, while the LDU algorithm defers only 49% of patients. This diagnostic task also illustrates a limitation of the direct triage by uncertainty algorithm: because the diagnostic entropy is zero for most patients (86%), the maximum defer rate for this algorithm is 14% and the corresponding maximum F1 score is 0.73.

These results suggest that even when the architecture of the underlying diagnostic network is relatively simple, the proposed LDU algorithm can lead to considerable gains in F1 score by deferring a smaller proportion of patients than learning to defer without uncertainty. Furthermore, the defer rate of the LDU algorithm is less sensitive than the direct triage algorithm to the distribution of predicted diagnoses (i.e. the diagnostic entropy) for each patient.

Diagnosis of pleural effusion and pneumothorax

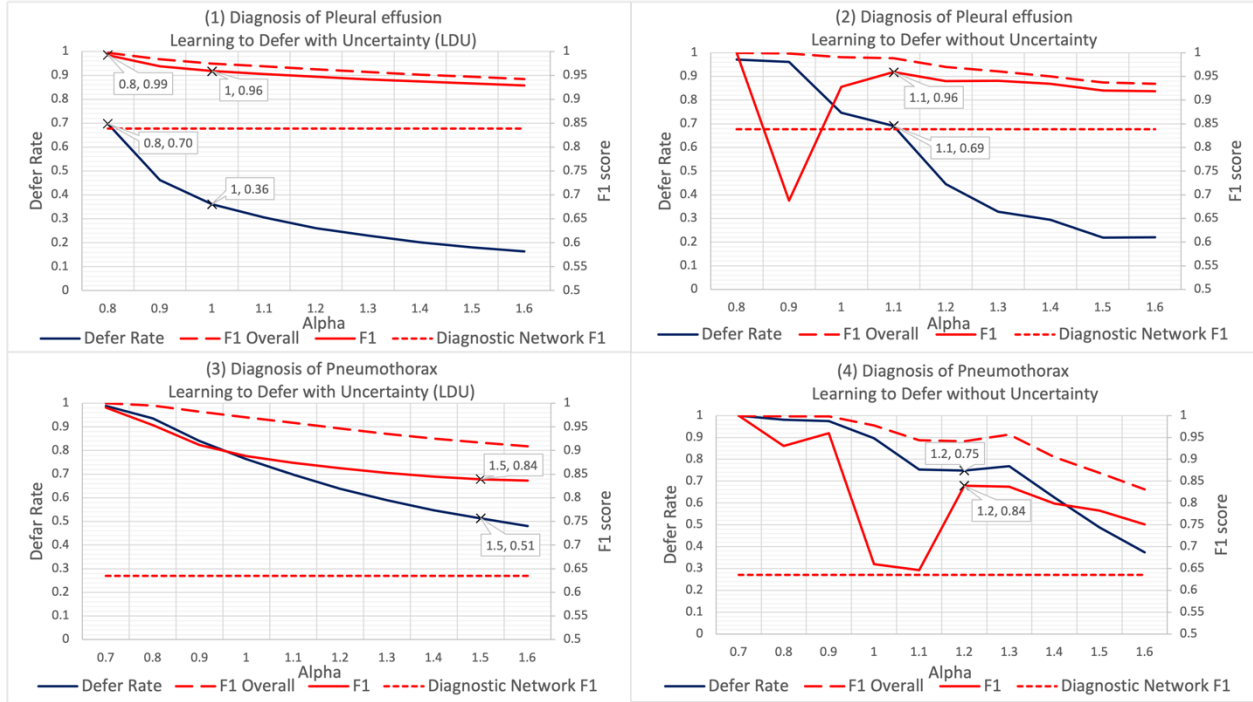


Figure 4. Performance comparison for the diagnostic tasks using MIMIC-CXR x-ray images: diagnosis of pleural effusion using (1) learning to defer with uncertainty (LDU) and (2) learning to defer without uncertainty information, diagnosis of pneumothorax using (3) learning to defer with uncertainty (LDU) and (4) learning to defer without uncertainty information. Each panel shows the F1 scores (red line) for patients who are not deferred to human experts, ‘F1 Overall’ scores (red dashed line) and the corresponding defer rates (blue line) for different values of the weight of the defer loss α . The diagnostic network F1 score (without the defer option) is 0.84 for pleural effusion, and 0.63 for pneumothorax (red dotted line).

Results for the image-based diagnostic tasks support previous findings using free-text and structured tabular data (Figure 4). In particular, the LDU algorithm defers less patients for human evaluation than learning to defer without uncertainty, while reaching the same F1 score. In the diagnosis of pleural effusion, to achieve an F1 score of 0.96 (14% increase over the diagnostic network’s F1 score), learning to defer without uncertainty defers 69% of patients while the LDU algorithm defers only 36% of patients. In the diagnosis of pneumothorax, to achieve an F1 score of 0.84 (a lower target than for pleural effusion because of the more difficult task, but a 25% increase over the diagnostic network’s F1 score of 0.63), the LDU algorithm defers only 51% of patients while learning to defer without uncertainty defers 75% of patients. The LDU algorithm is sufficiently accurate for a considerable proportion of patients even though the performance of a single underlying diagnostic network is poor.

In both diagnostic tasks, the F1 scores of the LDU algorithm increase monotonically as more patients are deferred to human experts.

α	Defer Rate	F1	Accuracy	Sensitivity	Specificity
0.77	81.91%	0.998	0.997	0.970	1.000
0.78	77.80%	0.996	0.994	0.980	0.998
0.79	73.64%	0.993	0.991	0.983	0.995
0.80	69.74%	0.992	0.990	0.984	0.994

Table 1. Performance metrics of the LDU algorithm in the diagnosis of pleural effusion, by setting the weight of defer loss between 0.77 and 0.80.

Furthermore, Table 1 shows additional performance metrics for the LDU algorithm when diagnosing pleural effusion and varying the weights α of the defer loss between 0.77 and 0.80. The LDU algorithm identifies about 18% to 30% of patients for whom the predicted diagnoses are almost certainly correct. This suggests that the LDU algorithm can identify a subgroup of patients for whom the diagnosis of pleural effusion can be automated with considerably low risk (the error probability can be controlled within 1%).

For both image-based diagnostic tasks, the diagnostic entropies are zero for all patients, i.e. the diagnoses predicted by the deep ensemble have different probabilities but all point to the same class. Therefore, direct triage by uncertainty cannot be directly applied to these tasks. Using the ensemble entropies instead of the diagnostic entropies does not lead to any increase in F1 scores either (Appendix B). In comparison, the LDU algorithm can achieve high F1 scores and low defer rates using only the probabilities predicted by the deep ensemble and their entropy.

Summary of Accuracy, Sensitivity and Specificity

Table 2 shows the defer rates of the LDU algorithm and learning to defer without uncertainty for selected F1 scores, as well as the corresponding accuracy, sensitivity and specificity metrics. The table suggests that the LDU algorithm results in better defer rates than learning to defer without uncertainty also when performance metrics other than F1 score are considered.

Data Source	Diagnostic Task	Method	F1	Defer Rate	Accuracy	Sensitivity	Specificity
MIMIC-III	Myocardial Infarction	Learning to defer	0.88	55%	0.84	0.70	0.93
		LDU	0.88	38%	0.90	0.94	0.84
Heritage Health	Comorbidity	Learning to defer	0.82	54%	0.81	0.79	0.83
		LDU	0.82	49%	0.80	0.76	0.85
MIMIC-CXR	Pleural Effusion	Learning to defer	0.96	69%	0.96	0.97	0.96
		LDU	0.96	36%	0.96	0.98	0.94
	Pneumothorax	Learning to defer	0.84	75%	0.76	0.42	0.94
		LDU	0.84	51%	0.83	0.85	0.82

Table 2. Comparison of accuracy, sensitivity, and specificity between the LDU algorithm and learning to defer without uncertainty for selected F1 scores, across all diagnostic tasks.

Discussion

In this study, we proposed a novel algorithm (learning to defer with uncertainty, LDU) which considers predictive uncertainty information when identifying patients who should be evaluated by human experts because computer-aided diagnosis is likely to be inaccurate. LDU was found to achieve similar F1 scores, but considerably lower defer rates, than a learning to defer method which does not consider uncertainty

information [6][7]. LDU was also associated with monotonic increases in performance and defer rates as the weight of the defer loss was decreased during training, suggesting that an optimal trade-off between LDU's performance and defer rate can easily be found for a variety of diagnostics tasks. On the contrary, learning to defer without uncertainty could not always guarantee increased performance as more patients were being deferred, making its performance in clinical settings somewhat unpredictable. Furthermore, for tasks such as the diagnosis of pleural effusion, the LDU algorithm was able to identify a subgroup of patients for whom the risk of an erroneous computer-aided diagnosis was close to zero. This might allow the application of computer-aided diagnosis even for diagnostic tasks where the cost of inaccurate predictions is high.

Unlike direct triage by uncertainty [2], LDU performed robustly even in situations where the deep ensemble predicted the wrong diagnosis with high confidence. We hypothesize that individual outlying predictions, which might not be noticeable when applying a simple threshold to the overall diagnostic entropy, are taken into account by LDU's 'learning to defer' neural network.

For the direct triage method, the maximum defer rate occurs at a threshold value of zero, which means that the defer rate can only be as large as the percentage of patients associated with non-zero uncertainty measures. This becomes problematic when a diagnostic network results in uncertainty measures of zero for a large portion of patients, and even more so if the uncertainty is zero for all patients (such as in the diagnosis of pleural effusion and pneumothorax). In these scenarios direct triage by uncertainty is bound to result in poor performance, but the LDU algorithm still led to a wide range of defer rates and large performance increases. Alternatively, we also tried using the ensemble entropy to triage patients, but this did not lead to any increase in performance (as described in Appendix B), because both correct and incorrect diagnoses can be associated with low entropy as a result of over-confident neural networks.

Both the LDU algorithm and the direct triage method rely on uncertainty measures to decide which patients should be deferred for human evaluation. Our current approach to capturing epistemic uncertainty is limited: for example, in the diagnosis of pleural effusion and pneumothorax the diagnostic entropy was zero for all patients, possibly due to overconfident predictions by networks in the deep ensemble. Future research could explore whether additional information about epistemic uncertainty could be captured by measuring the entropy of the outputs of intermediate network layers, rather than just of the softmax outputs, and evaluate Bayesian approaches to uncertainty quantification in deep neural networks. Further, this study only considered model uncertainty, and the cost of deferring a patient for human evaluation was assumed to be constant. This constraint is mainly related to the limited availability of public datasets with diagnostic labels from multiple human experts, which could be used to estimate the uncertainty of human diagnoses for each patient. If data with gold standard diagnoses and multiple human experts' labels for each patient were available, the LDU algorithm could be augmented to take into account both the model's and human uncertainty, and patients would be deferred for evaluation by human experts only if the human uncertainty was estimated to be lower than the model's uncertainty.

In conclusion, the proposed LDU algorithm can be used to mitigate the risk of erroneous computer-aided diagnoses in clinical settings. LDU identifies patients for whom the uncertainty of computer-aided diagnosis is estimated to be high and defers them for evaluation by human experts. The algorithm achieves similar diagnostic performance (F1 score, accuracy, sensitivity and specificity) to previous learning to defer algorithms but reduces the proportion of patients deferred for human evaluation. Furthermore, LDU's performance increases monotonically as more patients being deferred, suggesting that the desired trade-off between performance and defer ratio can be obtained for a wide variety of diagnostic tasks.

Appendix A. Diagnostic Neural Networks

Diagnosis of myocardial infarction

A BERT-based neural network was developed using an LSTM layer on top of bio discharge summary BERT [11]. The last output of the LSTM layer was passed through a fully connected layer with two outputs (for binary classification) and a sigmoid activation function [12][13]. Only the LSTM layer and the final fully connected layer were fine-tuned during training. The network was trained over 18 epochs using an ADAM optimizer with a learning rate of $1e-4$ and weight decay of 0.

Diagnosis of any comorbidities

For this task, we developed a fully connected neural network to predict whether a patient's Charlson Index was positive. The model had two hidden layers (each one with 200 nodes and a sigmoid activation function after the first layer) and two softmax-activated outputs. The model was trained over 4 epochs, again using an ADAM optimizer with a learning rate of $9e-4$ and weight decay of 0.

Diagnosis of pleural effusion and pneumothorax

A DenseNet121 model [15][16][17] was used for both diagnostic tasks after transforming and normalizing the input images. Both training processes used an ADAM optimizer with a learning rate of $1e-4$ and weight decay of $1e-5$. The network was trained over 2 epochs for the diagnosis of pleural effusion prediction, and over 4 epochs for the diagnosis of pneumothorax.

Appendix B

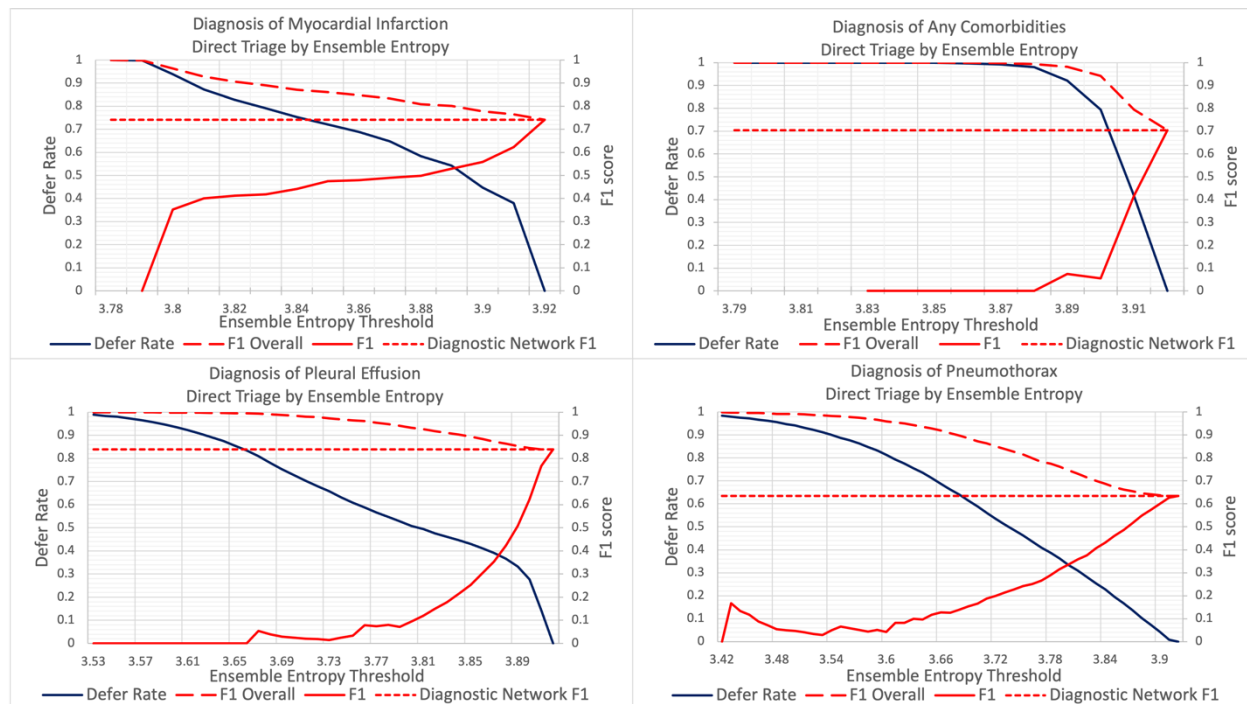


Figure 5. The results of the direct triage method by using a threshold value over the ensemble entropy, for the following tasks: (1) diagnosis of myocardial infarction, (2) diagnosis of any comorbidities, (3) diagnosis of pleural effusion and (4) diagnosis of pneumothorax. For each diagnostic task, the threshold

value (x-axis) varies between the minimum and the maximum ensemble entropy measured across the entire patient group. Each panel shows the F1 scores (red line) for patients who are not deferred to human experts, ‘F1 Overall’ scores (red dashed line) and the corresponding defer rates (blue line). The diagnostic network F1 scores (without defer option) are also shown for each task (red dotted line).

Figure 5 shows that ensemble entropy alone cannot be used as the triage score to select patient groups associated with high F1 scores, because the entropy of the continuous probabilities computed by a deep ensemble [9] can be low for both correct and incorrect predictions. Across all tasks, the F1 scores decrease, rather than increase, as more patients are deferred for evaluation by a human expert. The system’s overall F1 score increases with the defer rate only because human experts are assumed to make correct diagnoses for all deferred patients.

References

- [1] McKinney SM, Sieniek M, Godbole V, Godwin J, Antropova N, Ashrafian H, et al. International evaluation of an AI system for breast cancer screening. *Nature*. 2020;577(7788):89-94.
- [2] Raghu M, Blumer K, Corrado G, Kleinberg J, Obermeyer Z, Mullainathan S. The Algorithmic Automation Problem: Prediction, Triage, and Human Effort. March 01, 2019: [arXiv:1903.12220 p.]. Available from: <https://arxiv.org/pdf/1903.12220.pdf>.
- [3] Guo C, Pleiss G, Sun Y, Weinberger KQ, editors. On calibration of modern neural networks. *International Conference on Machine Learning*, PMLR. 2017.
- [4] Raghu M, Blumer K, Sayres R, Obermeyer Z, Kleinberg R, Mullainathan S, et al. Direct Uncertainty Prediction for Medical Second Opinions. July 01, 2018: [arXiv:1807.01771 p.]. Available from: <https://arxiv.org/pdf/1807.01771.pdf>.
- [5] Cortes C, DeSalvo G, Mohri M, editors. *Learning with Rejection*. Cham: Springer International Publishing. 2016.
- [6] Madras D, Pitassi T, Zemel R. Predict Responsibly: Improving Fairness and Accuracy by Learning to Defer. November 01, 2017: [arXiv:1711.06664 p.]. Available from: <https://arxiv.org/pdf/1711.06664.pdf>.
- [7] Mozannar, H, Sontag, D. Consistent Estimators for Learning to Defer to an Expert. In *Proceedings of the 37th International Conference on Machine Learning*. 2020.
- [8] Zhang X, Chen F, Lu C-T, Ramakrishnan N. Mitigating Uncertainty in Document Classification. July 01, 2019: [arXiv:1907.07590 p.]. Available from: <https://arxiv.org/pdf/1907.07590.pdf>.
- [9] Lakshminarayanan B, Pritzel A, Blundell C. Simple and Scalable Predictive Uncertainty Estimation using Deep Ensembles. December 01, 2016: [arXiv:1612.01474 p.]. Available from: <https://arxiv.org/pdf/1612.01474.pdf>.
- [10] Johnson AEW, Pollard TJ, Shen L, Lehman L-wH, Feng M, Ghassemi M, et al. MIMIC-III, a Freely Accessible Critical Care Database. *Scientific Data*. 2016;3(1):1.
- [11] Alsentzer E, Murphy JR, Boag W, Weng W-H, Jin D, Naumann T, et al. Publicly Available Clinical BERT Embeddings. April 01, 2019: [arXiv:1904.03323 p.]. Available from: <https://arxiv.org/pdf/1904.03323.pdf>.
- [12] Mulyar A, Schumacher E, Rouhizadeh M, Dredze M. Phenotyping of Clinical Notes with Improved Document Classification Models Using Contextualized Neural Language Models. October 01, 2019: [arXiv:1910.13664 p.]. Available from: <https://arxiv.org/pdf/1910.13664.pdf>.
- [13] Adhikari A, Ram A, Tang R, Lin J. DocBERT: BERT for Document Classification. April 01, 2019: [arXiv:1904.08398 p.]. Available from: <https://arxiv.org/pdf/1904.08398.pdf>.
- [14] Johnson AEW, Pollard TJ, Greenbaum NR, Lungren MP, Deng C-y, Peng Y, et al. MIMIC-CXR: A large publicly available database of labeled chest radiographs. *Nature Scientific Data*, 1 2019.

- [15] Rajpurkar P, Irvin J, Zhu K, Yang B, Mehta H, Duan T, et al. Chexnet: Radiologist-level pneumonia detection on chest x-rays with deep learning. November 1 2017: [arXiv:1711.05225 p.]. Available from: <https://arxiv.org/pdf/1711.05225.pdf>.
- [16] Huang G, Liu Z, Van Der Maaten L, Weinberger KQ, editors. Densely connected convolutional networks. Proceedings of the IEEE conference on computer vision and pattern recognition. 2017.
- [17] Dissez G, Duboc G. CheXpert : A Large Chest X-Ray Dataset and Competition. <https://github.com/gaetandi/cheXpert>